Journal of Civil, Construction and Environmental Engineering
2024, Vol. 9, No. 6, pp. 211-225
https://doi.org/10.11648/j.jccee.20240906.14

Research Article

Geotechnical and Geophysical Characterization of the Aklesal Dablyang Landslide: Implications for Slope Stability

Khomendra Bhandari[1, *], Mahendra Acahrya[2, *], Bhishma Joshi[1], Devendra Kumar Rokaya[3], Pawan Dumre[3], Suraj Belbase[1], Anil Ghimire[1], Sandesh Dhakal[1]

[1]Tri-chandra Multiple Campus, Department of Geology, Kathmandu, Nepal

[2]Department of Civil Engineering, Khwopa Engineering College, Bhaktapur, Nepal

[3]Department of Physics, Patan Multiple Campus, Lalitpur Nepal

Abstract

Landslides constitute one of the principal perils in Nepal, particularly within its hilly and mountainous terrains, where a confluence of geological fragility and climatic extremities engenders precarious landscapes. Such hazards precipitate considerable loss of life and property. This investigation centers on the Aklesal Dablyang landslide in Baglung district, a potent menace to local infrastructure, agricultural domains, and human lives. By deploying a synthesis of geotechnical (laboratory-based soil analysis) and geophysical (Electrical Resistivity Tomography (ERT)) methodologies, the intrinsic properties of the soil and rock substrata within the landslide precinct were meticulously examined. The findings reveal that the landslide comprises predominantly loose colluvial deposits with elevated moisture levels, resulting in reduced shear strength and heightened failure susceptibility. The study accentuates the pivotal influence of hydrological phenomena such as surface runoff and groundwater seepage in aggravating slope destabilization. These results underscore the exigency for efficacious risk mitigation strategies to diminish landslide impacts on vulnerable communities. The Aklesal Dablyang landslide exemplifies the intricate interplay of geological and hydrological dynamics within Nepal's complex topographical context. This research delineates the geotechnical and geophysical determinants of slope stability, highlighting the prevalence of loose colluvial deposits exacerbated by substantial moisture content, which attenuates shear strength and heightens vulnerability to mass movement. ERT analyses divulged a stratigraphy dominated by clayey sand interspersed with cobbles and boulders, which exhibit pronounced susceptibility to mass displacement during intense monsoonal precipitation—a phenomenon exacerbated by climate change. Anthropogenic interventions, including deficient drainage systems and substandard construction methodologies, further destabilize slopes by escalating pore-water pressure and diminishing soil cohesion. The study accentuates the imperative for integrative risk management paradigms, encompassing resilient engineering solutions, hydrological controls, and community collaboration, to bolster resilience against such geo-hazards.

Keywords

Electrical Resistivity Tomography, Grain Size Analysis, Infiltration, Landslide, Direct Shear Test

[*]Corresponding author: bhandarikhomendra@gmail.com (Khomendra Bhandari), acharyamahendra.tu.edu.nep2019@gmail.com (Mahendra Acharya)

Received: 5 October 2024; **Accepted:** 4 November 2024; **Published:** 28 November 2024

1. Introduction

The Himalayan region, which is characterized by high relief and intense monsoon rainfall, contributes to soil erosion and instability [9, 20]. As a result, approximately 12,000 landslide occurs annually in Nepal [2, 6]. Such hazards impact is beyond the immediate physical damage, as they pose severe risks to human life and infrastructures where communities are often situated near unstable slopes [4, 14]. According to the Ministry of Home Affairs (MoHA), Nepal experiences catastrophic landslides annually, causing hundreds of human casualties each year. These casualties from landslides alone account for about 25-30% of the total disaster-related fatalities in the country in various years [13]. Landslides, both new and reactivated, predominantly occur during the rainy season

The variation in lithology significantly influences the landslide susceptibility [7, 4] highlighted that highly weathered metamorphic rocks increase the risk of landslide due to their structural weakness. On the other hand, sedimentary rocks of the Siwaliks exhibit differential weathering, contributing to the slope failure [6, 10].

Geotechnical characterization of the landslides involves the assessing of the soil properties, i.e., including shear strength, cohesion, and moisture content [11]. The shear strength parameters of soil play a vital role in stability analysis. Cohesion and internal friction angle are essential parameters derived from the laboratory tests such as direct shear tests and triaxial tests [1, 16]. Research has shown that soils with low cohesion and high-water content are particularly susceptible to failure during the heavy rainfall [21, 19, 8] on the other hand emphasized on the importance of understanding the soil mechanics in the sedimentary terrains for predicting the landslide occurrences.

Geophysical methods have emerged as a valuable tool in recent years for the assessment of subsurface conditions related to landslides. Electrical Resistivity Tomography (ERT) and Ground Penetrating Radar (GPR) can provide insight into soil stratigraphy and water content distribution [3, 16, 16] demonstrated how ERT can effectively identify groundwater levels that influences the slope stability and utilized GPR for identification of potential slip surfaces. Similarly, [17] discussed the implication of using the satellite imagery for monitoring landslide in reservoir areas.

Understanding the geotechnical and geophysical characteristics of the Aklesal Dablyang landslide has significant implications for slope stability management. Effective risk mitigation stratigies can be developed by identifying critical factors that contribute to slope failure. The Aklesal Dablyang landslide in Baglung District is a particularly active and large landslide that poses a significant threat to road networks, agricultural land, and human settlements in the Dablyang area along the Maldhunga – Pagja – Paiyunpata - Kushmisera Road. The slope consists of colluvial deposits that are continuously moving downslope in parts, resulting in ongoing damage to agricultural land, forests, and roads. The size of the landslide is expanding, obstructing vehicle movement to the southern part of Baglung District, including the district headquarters and the Kali Gandaki Corridor Road, which connects the north and south of the district.

2. Study Area Location

The Aklesal Dablyang Landslide is located in Baglung Municipality, Ward-10, Baglung District, Gandaki Province, Western Nepal, at coordinates 28°14'57.13"N, 83°37'9.81"E (Figure 1). This landslide affects the newly constructed local road, which passes through the landslide area, with debris being transported to the Kali Gandaki River, exacerbating the situation through bank cutting. The landslide extends up to the river, and its slope is mainly covered by loose clayey sand with boulders and cobbles, occurring on a steep incline of loose colluvial deposits.

This recent landslide, situated at the edge of agricultural land facing the river, is caused by improper local road construction and gulley erosion during heavy rainfall. It spans approximately 35 meters wide at the top, 110 meters at the body, and 20 meters at the toe, with a length of about 450 meters from crown to toe. The hazard zone is around 60 meters wide at the top, 135 meters at the body, and 20 meters at the toe, extending 450-600 meters from top to bottom.

Currently, a few houses upslope and downslope of the landslide are not directly impacted, but the road is damaged annually, disrupting transportation due to debris flow. The expanding nature of the landslide suggests that some houses are at high risk in the future.

3. Methods and Methodology

3.1. Pre-Field Study

Field condition were analyzed through the study of images and maps. Additionally, related available documents and data was collected from various sources and studied to complete preliminary analysis. Satellite image was used for the study of morphology in and around the landslide area which was also used in conjunction with the digital elevation model and hill shade that was prepared from the digital topographic data of the Department of Survey. Similarly, geological and engineering geological information was extracted from the image which was helpful to further update and the existing geological map before the field visit. The tectonic setup and correlation of the major lineament in the area with the landslide was helpful to understand whether there is lithological or structural or hydro-meteorological control for the occurrence of landslide.

3.2. Field Investigation

After a meticulous analysis on pre-field data and detailed

methodological planning, various field data were collected using different tools and equipment such as; Compass/Clinometers, GPS, Geological hammer, ERT survey Equipment (GD-10 Supreme Resistivity Meter), Total Station, Measuring tape, field notebook, masking tape, marker pens, field camera, safety clothing, logistics etc. with detailed field investigations like aerial maps, topographic maps, aerial photographs and stereoscope were used in the field for verification of pre-field data an interpretations.

Preliminary survey of Alkesal Dablyang Landslide carried out through planned methodology which includes, walk through survey, measuring longitudinal and cross-sectional area of landslide by Total Station, noting dimension, orientation, rock types and other prominent features using geological compass, Google map, and topographic survey.

During this period of fieldwork, engineering geological investigations were done to collect detailed geological information around the landslide area. This included regional geological mapping, hazard map preparation, and identifying active landslide zones and causes of failure. Information regarding the slope condition, soil/rock distribution, extension and impact of slide material etc. were collected and suitable sites to construct mitigation measures like structures, its dimension and type of measure to be adopted were selected. Observations was also taken for proper management of drainage on and around the landslide area.

Assessment of the landslide area was carried out from geotechnical, hydrological and hydrogeological perspectives. The surface and subsurface water in the main landslide zone and surrounding area was mapped and their role in slope instability was assessed. Two soil samples were collected from the sites for test, the test result will be supportive in structural design.

Electrical Resistivity Method

Electrical resistivity method is based on ohms law and survey is done by injecting DC current into the ground through two electrodes and resulting voltage difference is measured. The apparent resistivity (ρa) is calculated from the current (I) and observed voltage difference (V) as follows:

$$(\rho a) = k\ V/I$$

The survey is carried out by passing DC electricity to the sub-surface and the electricity passes through the different layers underground as the electrical resistivity of rocks, sediments pores, fluid, joints, cracks, sheared joints etc. will experience different kinds of resistance, the potential difference is measured from the two electrodes placed on the surface. Hence, the sub-surface information was determined. Apparent resistivity values obtained in the field are not equal to the actual resistivity of the geologic units which affect the potential measured at the potential electrodes, unless measurements are being made over homogenous ground [18].

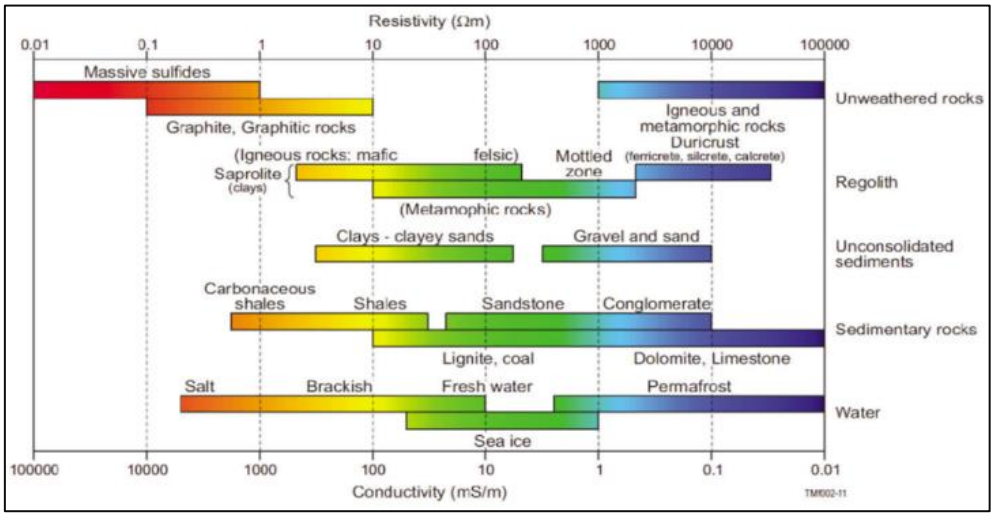

Figure 1. *Shows the conductivity-resistivity values of various rock-forming materials [12].*

The field data were filtered, processed and treated with the software, RES2DINV which inverts the data and calculates appropriate model and provides output in the form of resistivity cotours.

Infiltration Test

This test is done to measure the rate of water infiltration into the soil or other porous media. Single ring infiltrometer was used in the study. It involves driving a ring into the soil and supplying water into the ring either at constant head or falling head condition where supplying of water is done with a bottle. The infiltration test was carried out above the crown part and at the toe part. A HDPE pipe of length 60 cm (23) inches having diameter 4 inches was used. The pipe was inserted up to 15cm depth vertically into ground by striking top portion of the pipe as shown in figure 2.

Figure 2. *Field Infiltration test.*

Topographic survey

Topographical survey was carried out encompassing the entire landslide area and profile in 1:2500 scale depicting the tentative thickness and landslide's type was prepared. A topographical map of the active part of the landslide in scale 1:2000 was prepared showing critical locations.

Geological and Engineering Geological Mapping

The geological map showing lithology and structures, and engineering geological map showing the distribution of soil and rock, type and thickness of soil, physical properties of rocks with orientation of different set of discontinuities etc. are prepared. The entire landslide area was divided into several zones for purposing appropriate mitigation measures and based on geological, hydrological, engineering geological mapping and geophysical investigations of the area, it is classified on the basis of low, medium and high hazard zone.

Laboratory Tests

The samples were collected from the field and test such as; grain size distribution, natural moisture content (%), specific gravity, direct shear test were carried out to determine properties of the soil material of landslide area.

HYDROLOGICAL ANALYSIS

Risk analysis

Risk analysis was conducted to understand natural or in-built uncertainty, including hydrological risk of failure for drainage structures (graph is shown in the figure 3). The risk (R) is a function of return period of the design flood (T) and the expected life of the structure (n) and is given by:

$$R=1-(1-1/T)^n$$

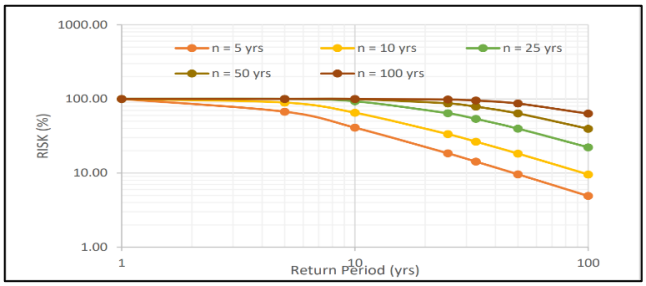

Figure 3. *Risk analysis Graph for Drainage structures.*

The frequency or return period of design flood is determined with the basic consideration of the risk involved and cost of minimizing that risk. The risk factor depends on the type and size of the structure, the volume of water passing through it, and the potential damage in the event of failure, which is influenced by the population and property downstream that could be affected by the worst-case scenario.

Geology and Engineering Geology

Previous geological data were obtained from the Department of Mines and Geology [5], which compiled information from the western region of Nepal and from [15] geological map of the lesser Himalaya in the Kushma-Baglung area.

Detailed geological mapping was carried marking 36 locations and detailed analysis was conducted based on the observation and measurements. The slide is developed in the rocks of quartzite and phyllite of the Kushma Formation, Lesser Himalaya which can be correlated with the Kunchha Formation and Fagfog Quartzite of the Central Nepal Lesser Himalaya. The upper slope consists of thick layer of ill sorted, loose, fine to coarse colluviums consisting of 50-60% boulders, 30% pebbles and cobbles, 10-20% fine soil with no bedrocks in the middle and toe part of slide. Geological mapping involved marking key locations across the landslide area, focusing on the crown, slope, and toe. Unmanaged surface drainage, bedrock at the crown, and colluvial deposits with well-developed gullies below were seen. The whole area of Aklesal Dablyang Landslide is located in slope with highly fragile, loose soil mostly boulders which is prone to landslide, slope failure and debris flows. Number of landslides and slope failures was observed in the periphery of the landslide area.

Slope stability condition

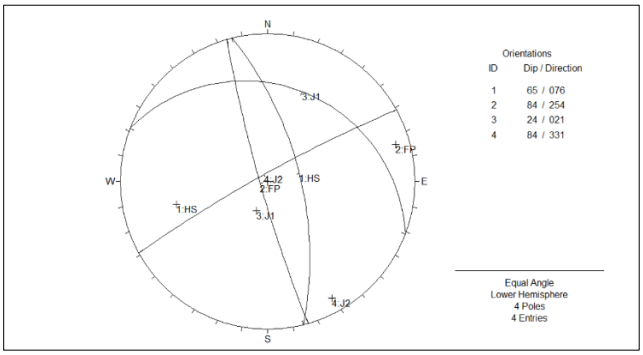

Figure 4. *Stereographic projection of Rock mass at slide area.*

Slope stability in the bedrock was analyzed using stereographic projection, based on the field data of major discontinuities, including the natural hill slope, which were plotted on a stereonet. The wedged formed by intersection of joints (J1 and J2) seems to be critical and there is possibility to occur the plane failure along the joint (J1). Other remaining wedges seems to be stable (Figure 4).

4. Results and Findings

4.1. Engineering Geology

The main part of the landslide is 35m wide at top part, 110m wide at body part, 20m wide at the toe part and about 450m long from crown to toe, with small channel of height difference 25m in 450 with an angle of 35-45 degrees is running in the middle with sloping land (about 30-60 degrees) at both sides.

The major cause of the landslide is weak geological setup, steep slope along with seepage water from gulley developing pore-water pressure that decreases the soil strength. The slope materials consists mostly of fine colluvial deposit with cobbles and boulders which is highly loose and fragile in terms of strength. Tap water from the houses directing toward landslide area and recent construction of the local motorable road further destabilized the slope. During rainfall, surface runoff from the catchment concentrates on the landslide, while seeping tap water increases its vulnerability to landslides and slope failure. A hazard map (Figure 8) and engineering geological maps (Figure 4, Figure 5, Figure 6) are prepared considering parameters like landslide scar, presence of tension cracks, slope of the area, vegetation surface and groundwater activities, material type etc.

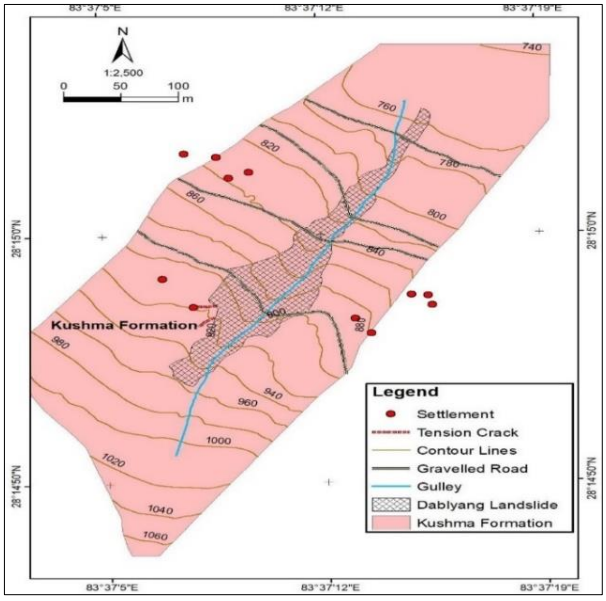

Figure 5. *Geological map of study area.*

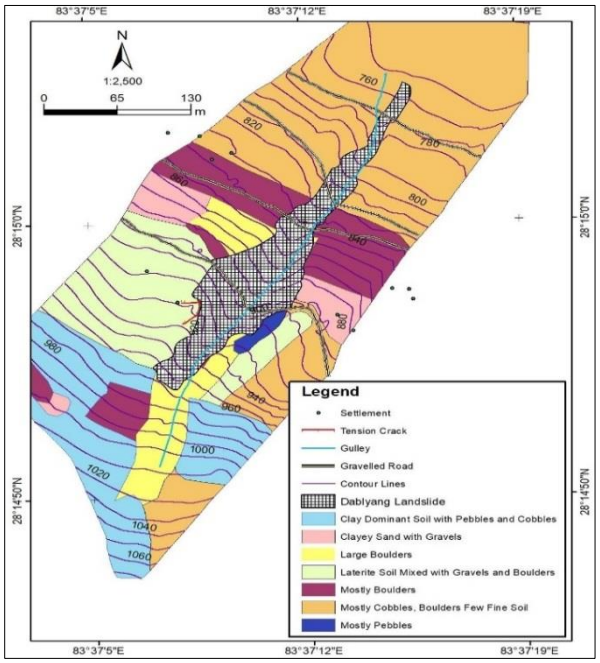

Figure 6. *Engineering geological map of study area.*

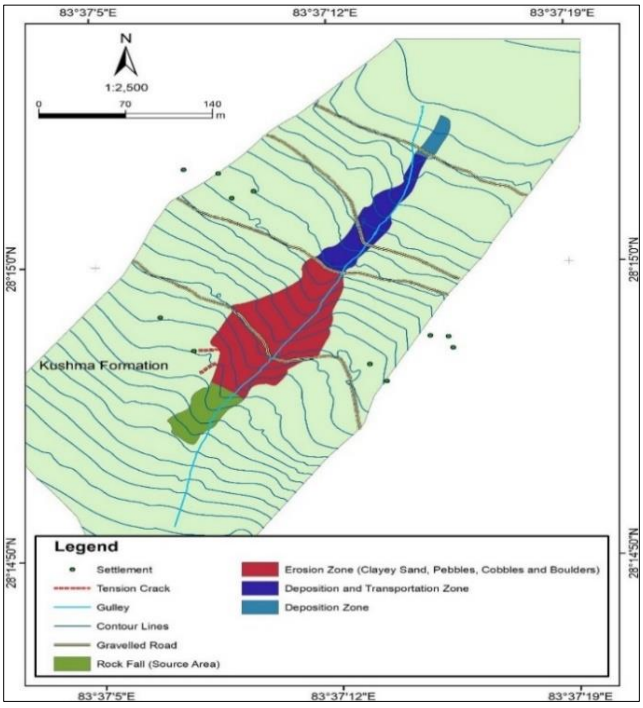

Figure 7. *Rock and soil distribution map of study area.*

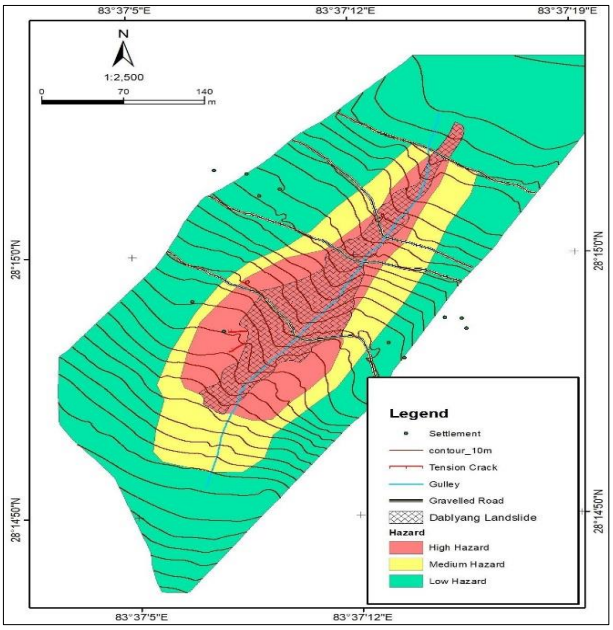

Figure 8. *Field based hazard map of study.*

4.2. Relationship Between Earthquake and Alkesal Dablyang Landslide Occurance

The study of earthquake activity around the Aklesal Dablyang Landslide between May 1 and May 20, 2021 (as shown in Figure 10), found no earthquakes above.

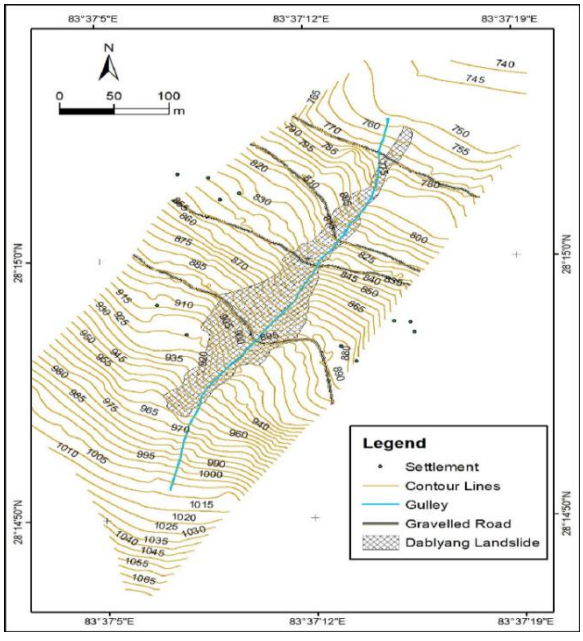

Figure 9. *Topographic map of landslie.*

Magnitude near the site, and those below 4 magnitude had epicenters over 100 km away. Suggesting the earthquake does not have direct impact on the landslide.

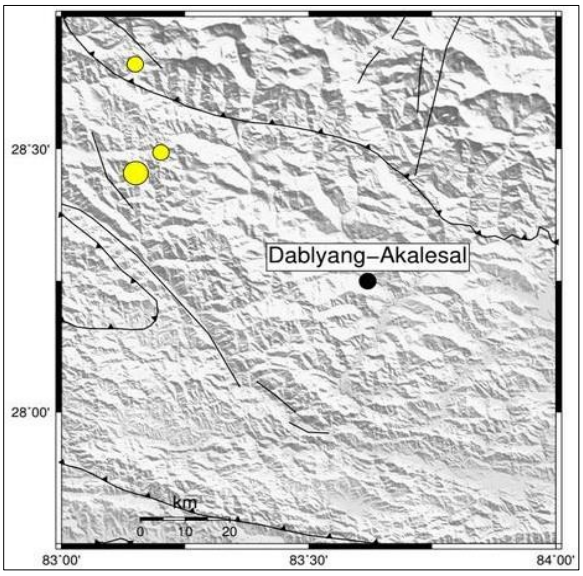

Figure 10. *Topographic map of landslie.*

4.3. Engineering Survey

The topography survey for acquiring field data was carried out to find out contour lines and exact location of landslide. The topographical map was prepared as shown in the Figure 9 and from topographic map, aspect map (Figure 10), hillshade map (Figure 11) slope map (Figure 12) and elevation map (Figure 13) were prepared.

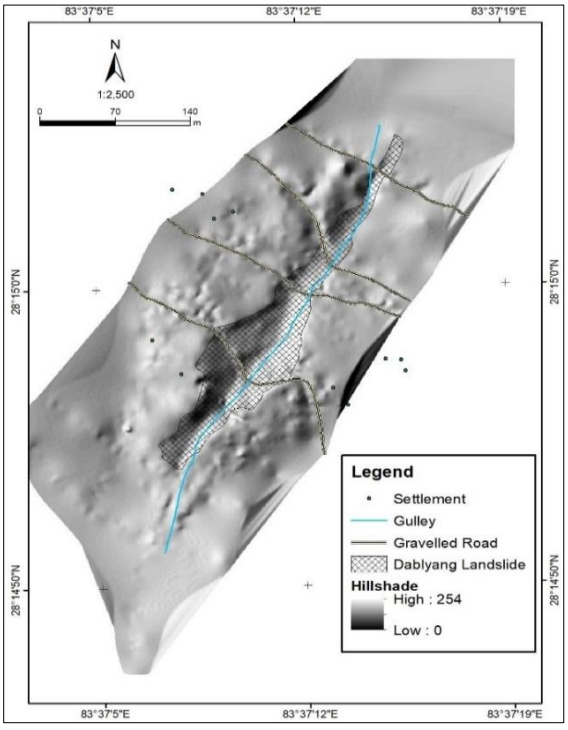

Figure 11. *Occurrence of Earthquake below 4 magnitude Richter scale around Aklesal Dablyang Landslide between May 1 to May 20, 2021.*

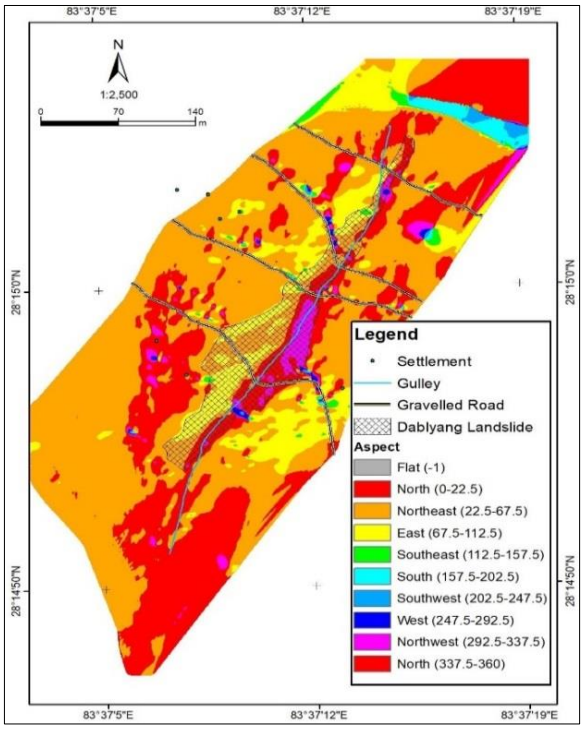

Figure 12. *Hillshade of landslide*

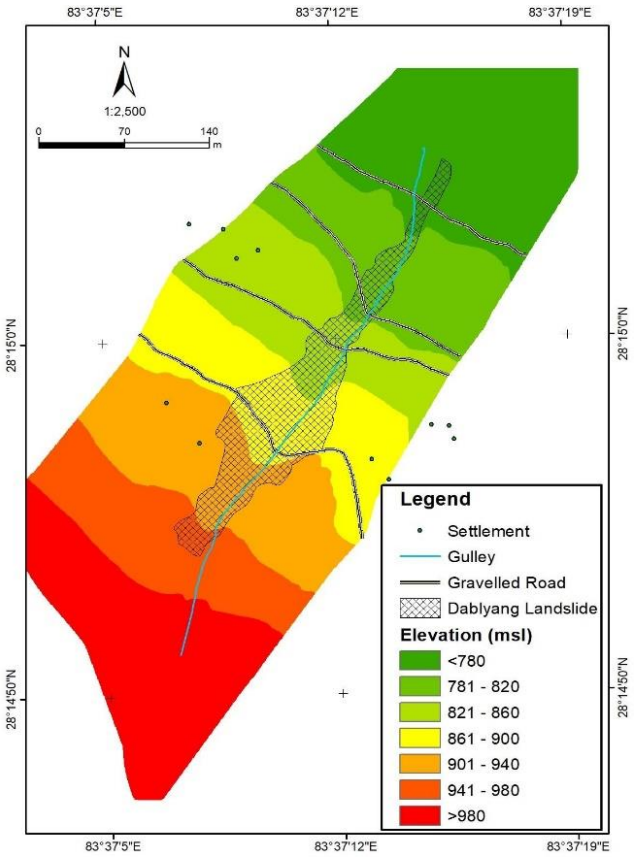

Figure 13. *Slope map of landslide.*

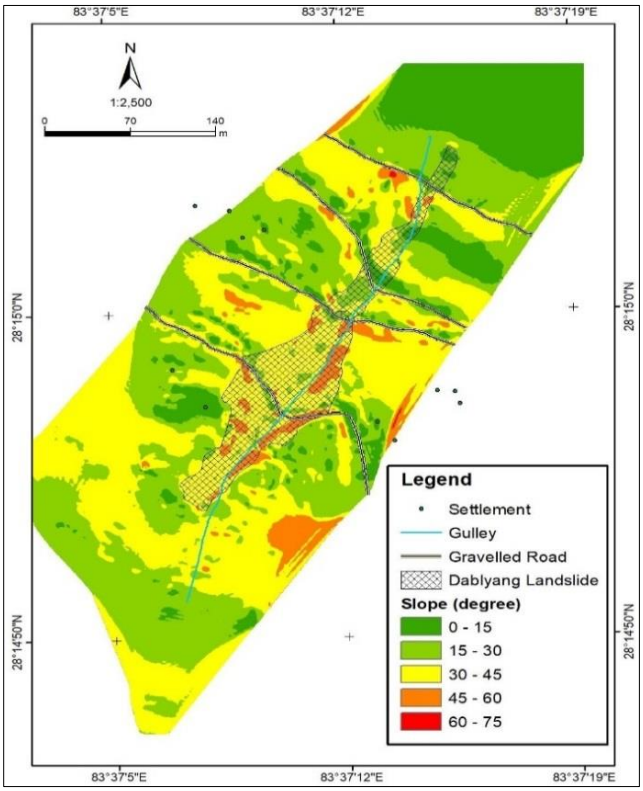

Figure 14. *Elevation map of landslide.*

4.4. 2D Electrical Resistivity Tomography

To understand the surface condition of the area, 4 profiles were proposed in the study area but based on the site condition 10

ERT survey were carried out at 10 different section in the landslide crown part, transportation part and deposition part to understand subsurface condition of the landslide in detail.

Resistivity Tomogram and lithological Interpretation of ERT-1

This profile extends 245 m from southeast to northwest with 5 m electrode spacing, and the lithology is interpreted as three-layered model. Top layer indicates colluvial deposit with sand, gravels and boulders with layer thickness of 3 m to 10.5 m across different chainages, gravels, sand and boulders with layer thickness from 9 m to 17 m. Second layer indicates fractured rock at depth of 8.8 m and 11 m, sand and gravels with thickness ranging from 2m to 8.5m, fine colluvial deposits, with thicknesses from 8 m to 12.5 m, hard, competent bedrock at depths of 11 m and 12 m, and colluvial deposits of gravels and boulders, with thicknesses of 9.5 m to 12.5 m. Third layer indicates fractured bedrock at depth of 12.5 m to 19 m and hard and competent bedrock with depth varies from 16 m to 23.5 m. (Figure 15).

Resistivity Tomogram and lithological Interpretation of ERT-2

This profile runs 395 m from upslope and ending towards downslope, and lithology is interpreted as four-layered model. Top layer demonstrate colluvial deposits with mostly gravels

with thickness varying from 4.5 m to 18 m aling different chainages, fine colluvial deposit with thickness ranging from 2 m to 6.5 m, gravels and boulders with thickness 2.5 m to 12.5 m, fine colluvial deposit at depth varying from 3 m to 13.5 m. Second layer indicates fractured bedrock at expected depth of 12.5 to 13.5 m, colluival deposit with mostly gravels with layer thickness 5 m to 12 m, and hard and comptent bedrock at depth at 3 m and 9.5 m. Third layer indicates fractured bedrock at expected depth of 12.5 m to 26 m, hard and competent bedrock with layer thickness ranges from 12.5 m to 36.5 m. Fourth layer indicates hard and competent bedrock with thickness ranges from 12.5m to 36 m. (Figure 16)

Resistivity Tomogram and lithological Interpretation of ERT-3

This profile of length 195 m with 5 m spacing between the electrodes run across the profile from southeast and ending towards northwest. Representative resistivity tomogram and its interpretation is shown in the figure. The lithological section is interpreted as multi layered model. Top layer with resistivity value below 650 Ωm from start of profile to chainage 67 m, chainage 105 m to 120 m and chainage 137 m to 161 m indicates fine colluvial deposit, with layer thickness varying from 2 m to 13.5 m. Resistivity value between 652 Ωm -1080 Ωm from chainage 14 m to 172 m indicates colluvial deposit with mostly gravels, with thickness thickness ranging from 3.5 m to 18m and resistivity ranging 1500 Ωm-1742 Ωm indicates colluvial deposits with boulders. Second layer with resistivity value above 1080 Ωm indicates bedrock with depth varying from 4.5 m to 15.5m

Resistivity Tomogram and lithological Interpretation of ERT-4

The profile extends 195 m from southeast to northwest with 5 m electrode spacing, and the lithology suggests a multi-layered model. Top layer indicates fine colluvial deposit with layer thickness 4.8 m and 9.5 m, followed by deposits with gravels and boulders in thickness 5.5 m to 7.8 m, layer of cobbles and pebble with thickness 6.5 m to 13 m, and a competent bedrock layer with a thickness of 4.2m. Second layer indicates fine colluvial deposit with a layer thickness 10.5 m to 17 m at a depth ranges from 2 m to 6m, competent bedrock at depth varying from 5m to 8m, colluvial deposit mostly cobbles and pebbles with layer thickness 10 m, fine colluvial deposit with layer thickness 8 m and 9m.

Third layer shows competent bedrock at the depth varying from 8 m to 25.5 m. (Figure 18)

Resistivity Tomogram and lithological Interpretation of ERT-5

The profile extends 245 m from southeast to northwest with 5 m electrode spacing, and the lithology suggests a multi-layered model. Top layer indicates colluvial deposit with gravels and boulders with a ;ayer thickness ranges from 4 m to 9.5 m.

Second layer stipulate bedrock at varying depth from 4 m to 6 m, fractured bed rock at depth 6.5 m, fine colluvial deposit with layer thickness ranging from 4 m to 9.5 m at a expected depth of 165 m to the end of the profile and colluvial deposits with mostly gravels with layer thickness of 7m and 9.5 m. Third layer shows fractured bedrock at expected depth ranging from 13 m to 14.5 m, colluvial deposits with mostly gravels with layer thickness varying from 1.5 m to 2 m. Fourth layer indicates bedrock at exected depth ranging from 16 m to 18 m, fractured bedrock at the 16 m to 20 m. Fifth layer shows bedrock at depth ranging form 18.5 m to 22m. (Figure 19).

Resistivity Tomogram and lithological Interpretation of ERT-6

The profile extends 245 m from southeast to northwest with 5 m electrode spacing, and the lithology suggests a mlti-layered model. Top layer indicates colluvial deposits with gravels and boulders, with layer thickness varying from 1.5 m to 11.5 m. Second layer indicates colluvial depostis with mostly boulders, with layer thickness varying from 7.5 m to 12.5 m, fine colluvial deposits, with layer thickness varying from 4.5 m to 12 m. Third layer dipcits fractured bed rock at expected depth of 11.5 m to 23 m. Fourth layer indicates hard and competent bedrock at expected depth of 14.5 m to 29.5 m. (Figure 20)

Resistivity Tomogram and lithological Interpretation of ERT-7

The profile extends 245 m from upslope to downslope with 5 m electrode spacing, and the lithology suggests a three-layered model. Top layer indicates fine colluvial deposit, with layer thickness varying from 2.5 m to 5 m, colluvial deposits with gravels and boulders, with layer thickness of 8 m to 15 m, colluvial deposit with sand, gravel and boulder, with layer thickness of 5 m to 10 m. Second layer indicates colluvial deposit with gravels and boulders at expected depth of 2.5 m to 5.5 m, fine colluvial deposit with layered thickness of 10 m and 9 m and, colluvial deposit with sand and gravel withlayer thickness 6.5 m to 17 m. Third layer shows bedrock at expected depth of 17 m to 23.5 m and fractured bedrock at depth of 12.5 m to 28.5 m. (Figure 21)

Resistivity Tomogram and lithological Interpretation of ERT-8

The profile extends 380 m from upslope to downslope with 5 m electrode spacing, and the lithography indicates a four-layered model. Top layer indicates boulder and gravels with layer thickness of 3.5 m to 17 m.

Second layer shows colluvial deposits with mostly gravels with layer thickeness of 2 m to 15.5 m, patches of fine colluvial deposit with layer thickness of 5 m to 15 m and fractured rock at depth of 13.5 m to 16 m. Third layer indicates fractured bedrock at depth of 16 m to 24 m and fourth layer shows bedrock at expected depth of 20 m to 34.5 m.

Resistivity Tomogram and lithological Interpretation of ERT-9

Profile runs 245 m from upslope towards downslope with 5 m electrode spacing, and the lithography indicates a three-layered model. Top layer indicates colluvial deposits with mostly gravels having layer thickness of 1.5 m to 11 m,

fine colluvial deposits with layer thickness of 4.5 m to 11 m. Second layer indicates competent bedrock with layer thickness of 7 m to 13 m and third layer indicates fractured bedrock at expected depth of 13.5 m to 38 m. (Figure 22).

Resistivity Tomogram and lithological Interpretation of ERT-10

This profile runs 195 m from southeast towards northwest with 5 m electrode spacing and the lithograpgy indicates two-layered model. Top layer indicates gravels and boulders with layer thickness of 5 m to 12.5 m and colluvial deposit with mostly gravels with layer thickness of 8 m to 16 m. Second layer indicates weathered and fractured bedrock at expected depth of 12.5 m, 13 m and at 10m, bedrock at expected depth of 8 m, 9 m and at 16 m, and fractured bedrock at expected depth of 14 m, 8 m and at 5 m of varying chainage. Following are the multilayered lithographic model at different locations of Landslide area. (Figure 23)

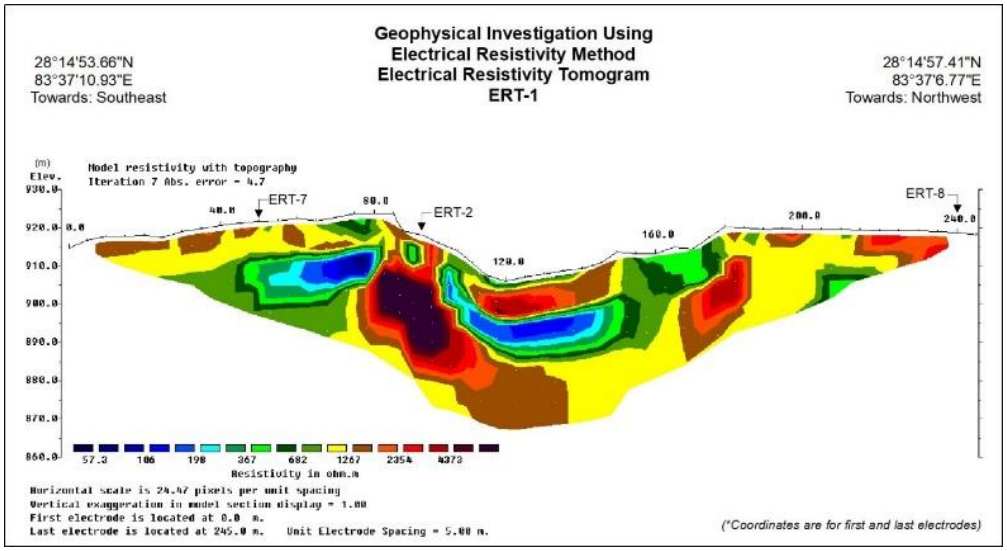

Figure 15. *Electrical Resistivity Tomogram of ERT-1.*

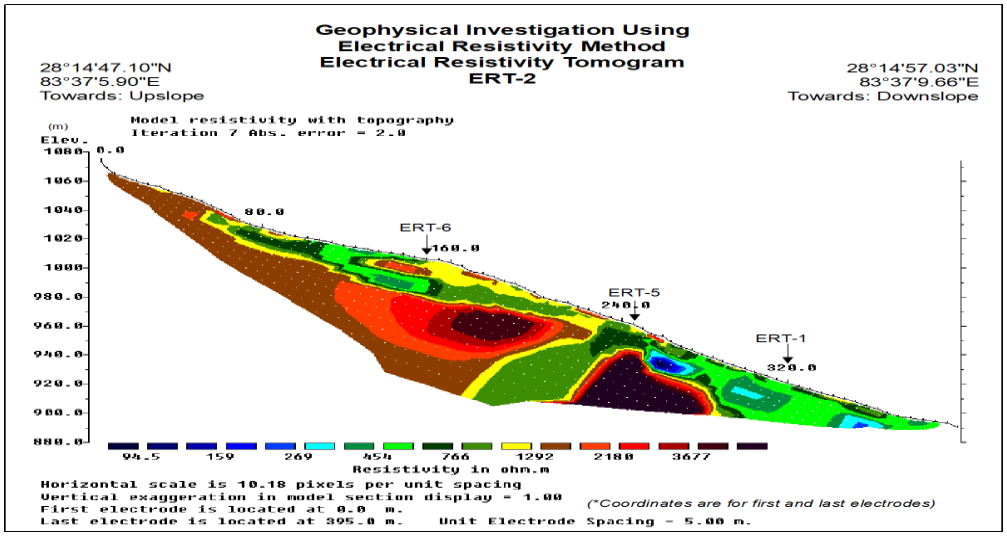

Figure 16. *Electrical Resistivity Tomogram of ERT-2.*

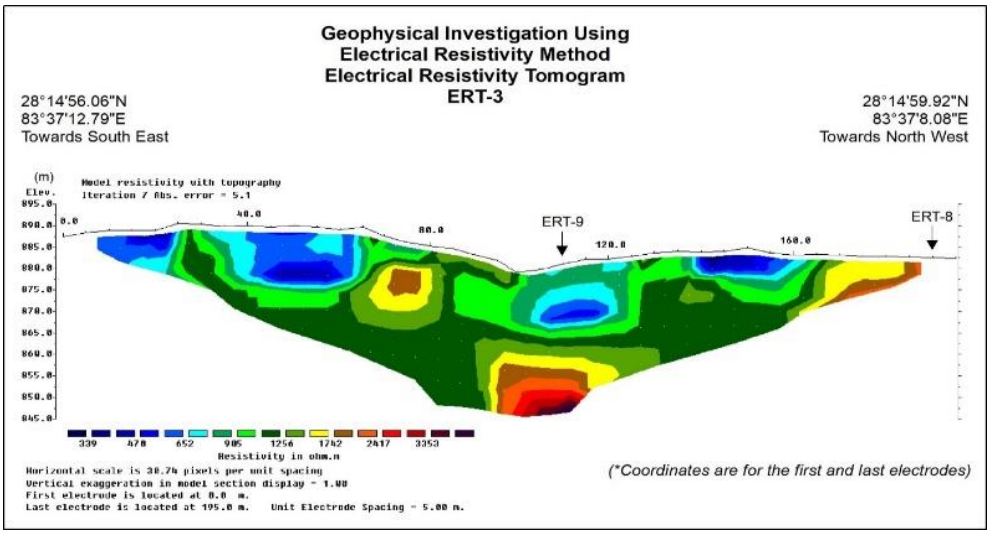

Figure 17. *Electrical Resistivity Tomogram of ERT-3.*

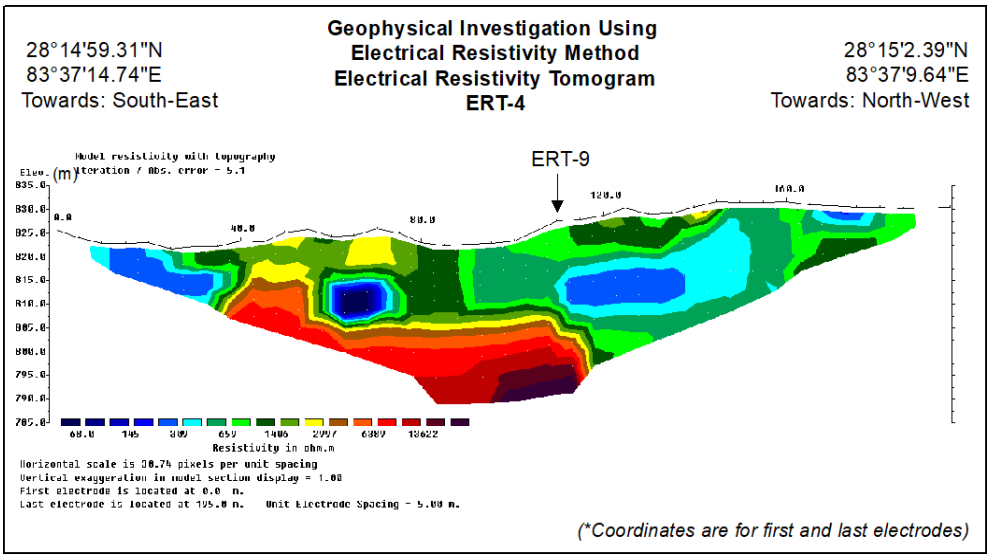

Figure 18. *Electrical Resistivity Tomogram of ERT-4.*

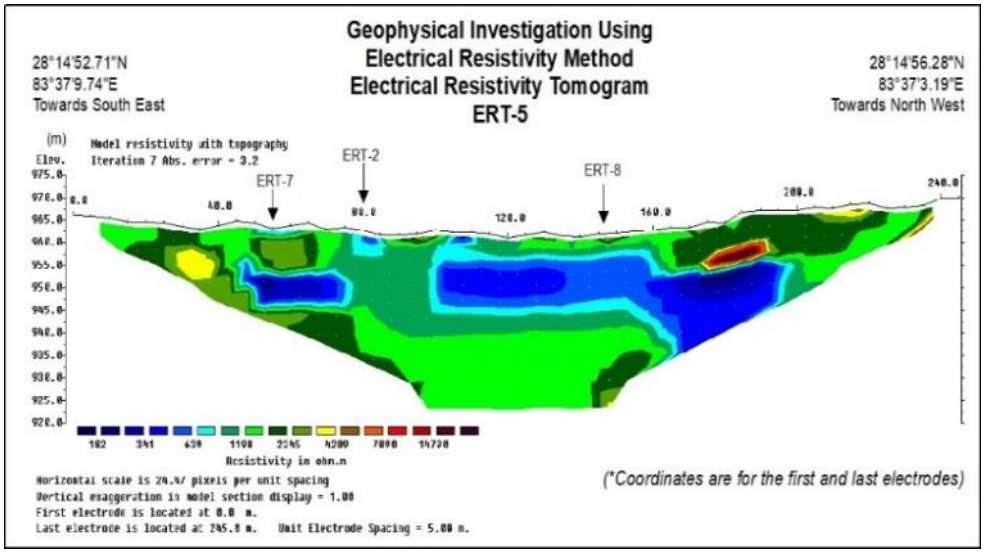

Figure 19. *Electrical Resistivity Tomogram of ERT-5.*

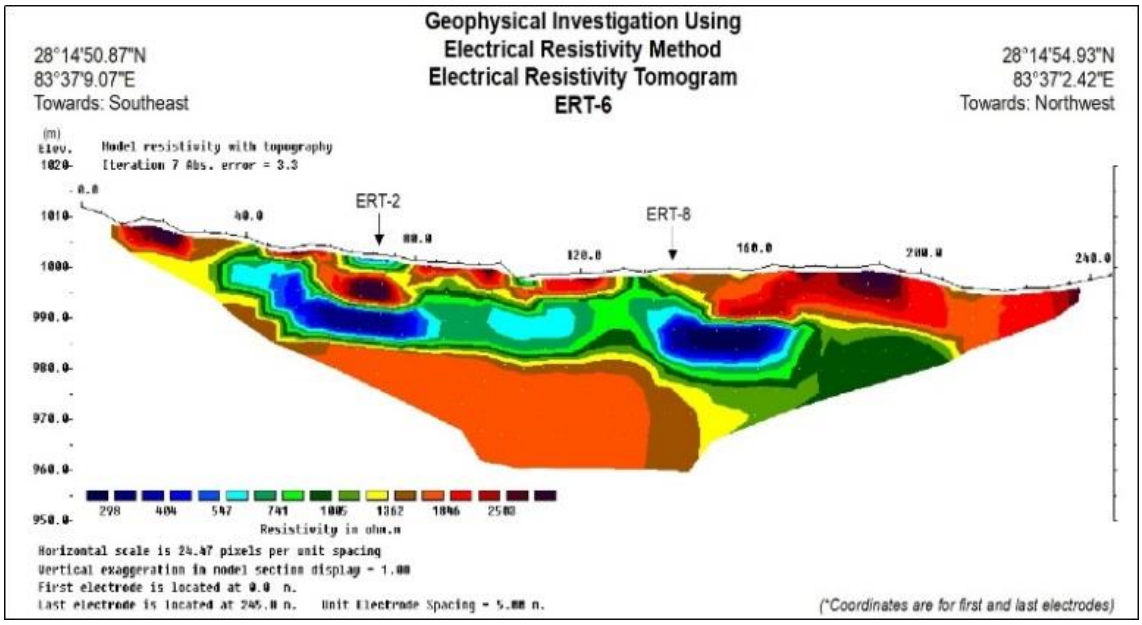

Figure 20. *Electrical Resistivity Tomogram of ERT-6.*

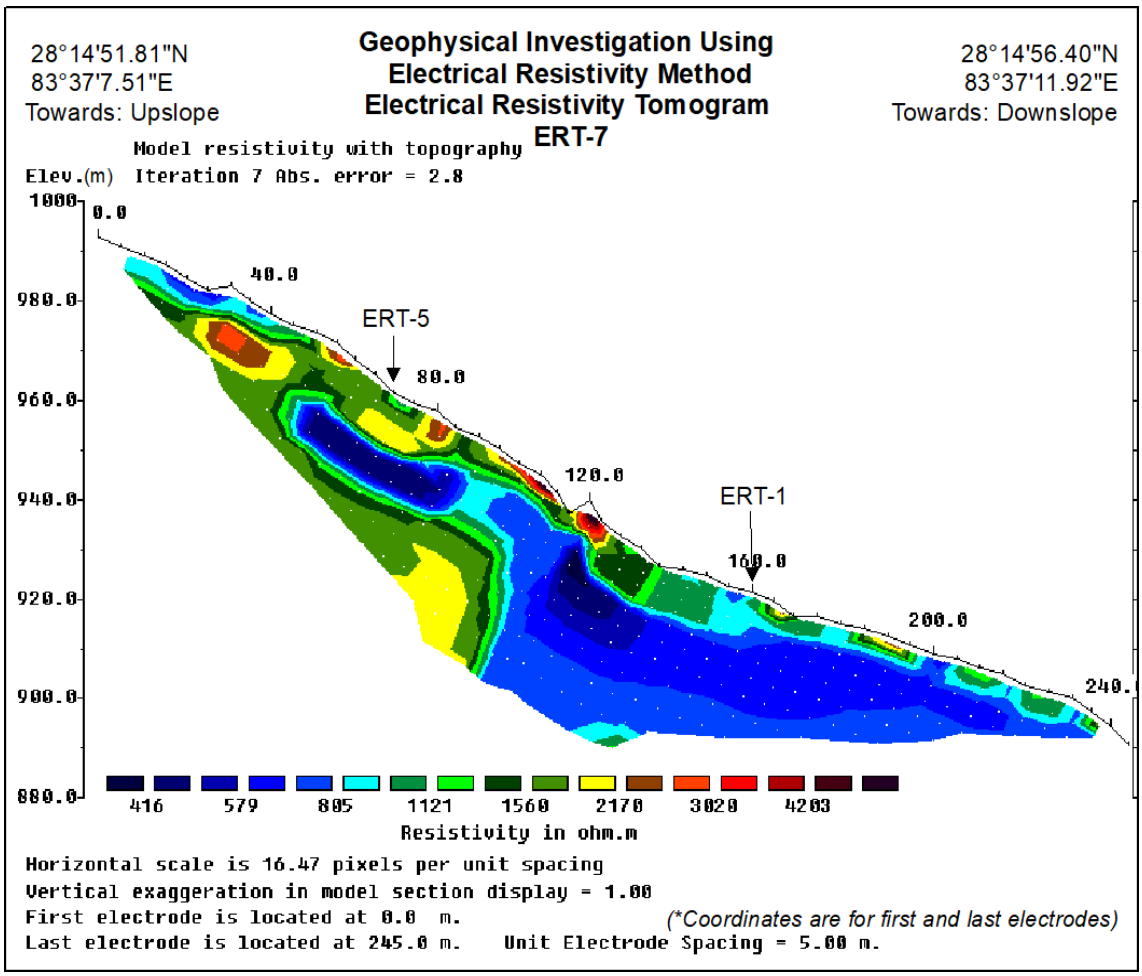

Figure 21. *Electrical Resistivity Tomogram of ERT-7.*

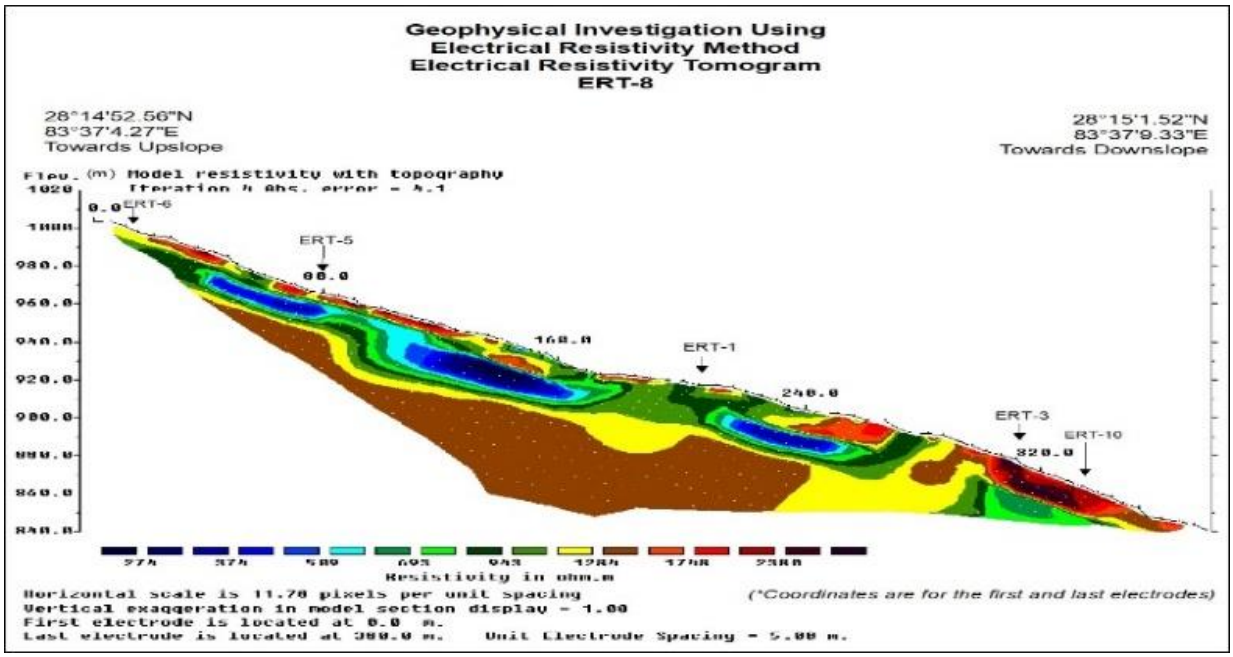

Figure 22. Electrical Resistivity Tomogram of ERT-8.

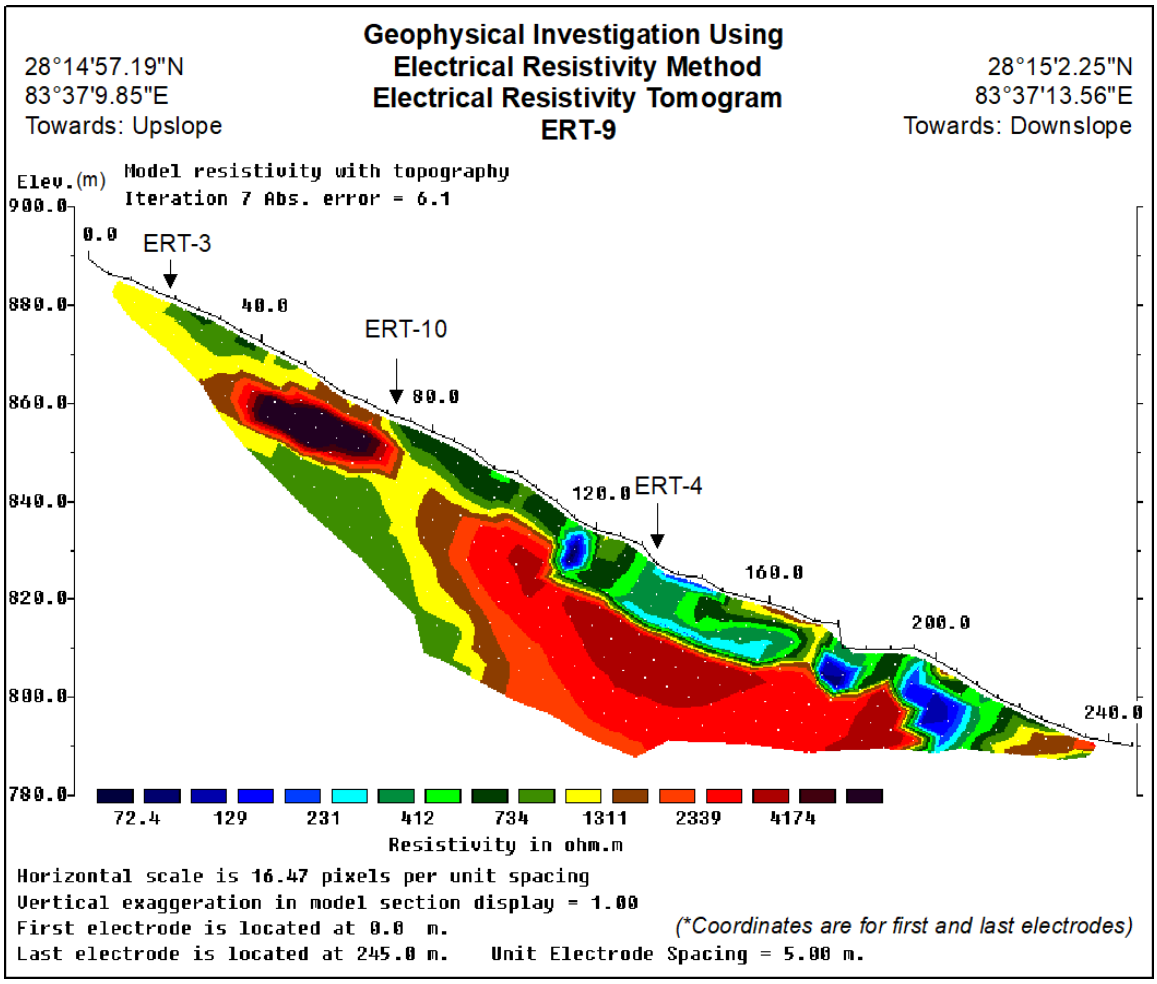

Figure 23. Electrical Resistivity Tomogram of ERT-9.

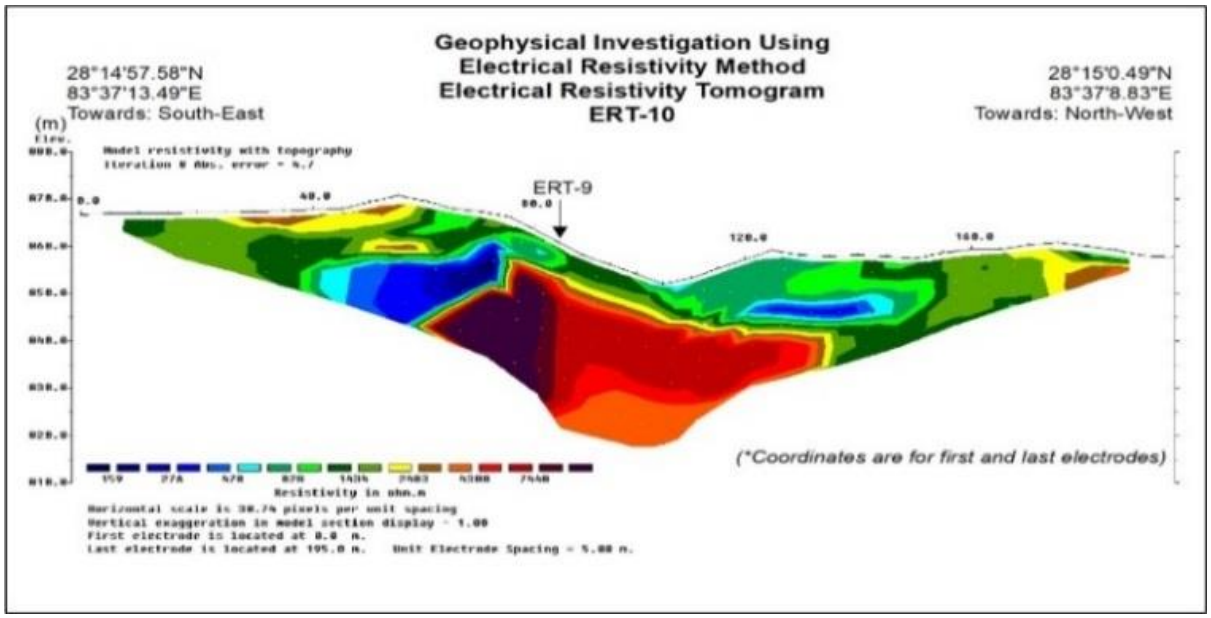

Figure 24. Electrical Resistivity Tomogram of ERT-10.

4.5. Laboratory Tests Results

Grain Size Analysis and Direct Shear Test

The grain size distribution curve (Figures 25 and 27) for the soil samples obtained from DL Upper part-1 and DL Lower part-2 of Dablung- Akisel Landslide were obtained through IS: 2720 (Part 4)-1985 standard method. The laboratory test results shows that the friction angle (φ) 33-34 °, and cohesion (c) 3-5 KN/m2 from the graph (Figure 26, Figure 28). The composition of the soil contents of clay 4.5-6.3%, silt 6-8%, sand 43-36% and gravel 47-50%. The natural moisture content ranges from 8 to 10% and specific gravity ranges from 2.64-2.65.

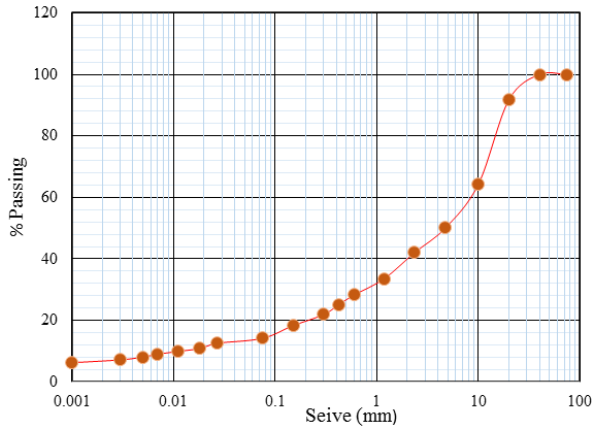

Figure 25. Grain size distribution of sample (DL Upper part-1).

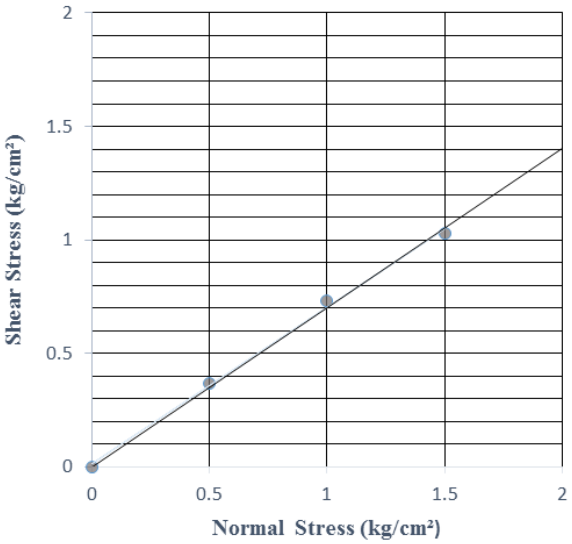

Figure 26. Grain size distribution of sample (DL Lower Part-2).

Direct Shear Test

Direct shear test was conducted to determine cohesion and internal friction angle of the samples. The sample obtained from DL Upper Part 1 shows the angle of internal friction 33^0 and cohesion $5kg/cm^2$ while, the result from Dl Lower Part-2 shows internal angle of friction 34^0 and cohesion of $3kg/cm^2$.

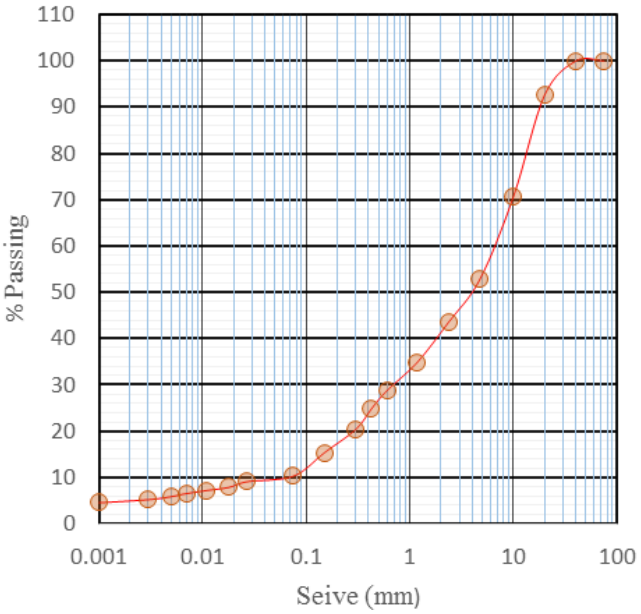

Figure 27. *Result of direct shear test of sample (Dl upper Part-1).*

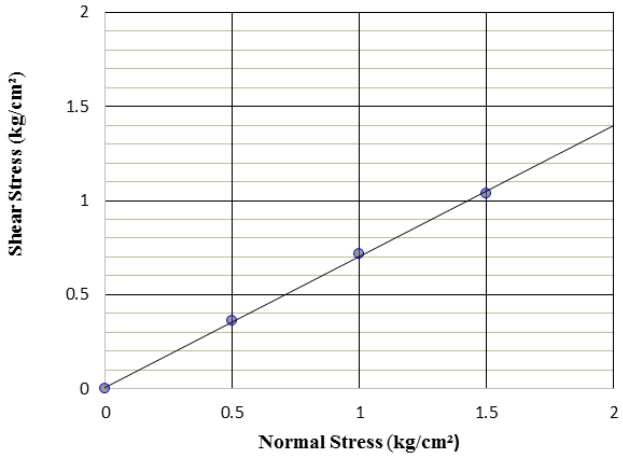

Figure 28. *Result of direct shear test of sample (DL Lower part-2).*

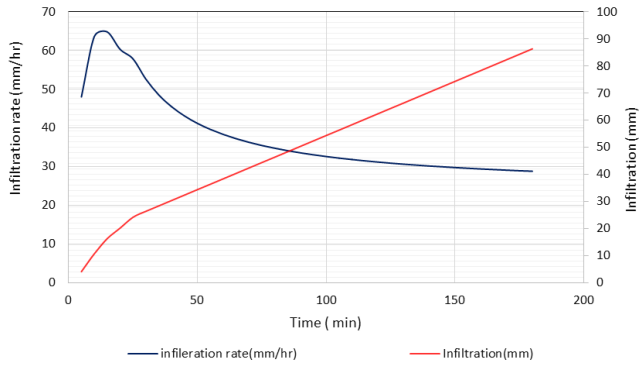

Figure 29. *Infiltration rate and infiltration depth at different time interval at location 1.*

Infiltration Test

Infiltration (in mm) for 3 hours at different time intervals was measured at two different location and maximum infiltration rate at location-1 was obtained 64.8 mm/hr in 15 minutes (Figure 29) and at location-2 was obtained 216 mm/hr in 5 and 10 minutes(Figure 30).

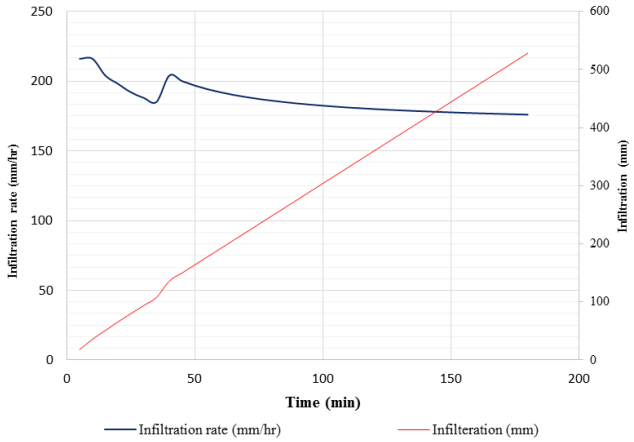

Figure 30. *Infiltration rate and infiltration depth at different time interval at location 2.*

5. Discussion

The Aklesal Dablyang landslide can be considered as a compelling case study for understanding the landslide dynamics in Nepal. The geotechnical analysis reveled that the landslide's composition is primarily loose colluvial deposits. The high moisture content observed during the field investigation aligns with the previous studies that emphasizes role of water infiltration in triggering landslides [3, 20]. The ERT results reveals that the top layer predominantly consists of loose clayey sand with boulders and cobble. These are highly susceptible to erosion and mass movement during heavy rainfall events [7]. It is particularly concerning, as the intensity of monsoon rains attribute to climate change. This has shown to worsen the landslide occurrence in similar geological settings [6]. Observations regarding surface runoff and improper drainage practices shows how anthropogenic factors compound to natural vulnerabilities. Flow of water from local sources leading towards the landslide area further activate the slope during.

6. Conclusion

The research provides overview into the geotechnical and geophysical characteristics that influences the stability of Aklesal Dablyang landslide. Key factors such as high moisture content and loose colluvial deposits urges the need for effective risk management as it have significantly diminished shear strength and increased the susceptibility to failure. These findings have signified the importance of understanding the hydrological dynamics affecting the

slope stability, particularly during the monsoon season, when heavy rainfall amplify the landslide occurrences. Human activities, such as improper drainage practices and construction methods have also played the significant role in destabilizing slopes. Flow of water from local (domestic) sources increases the pore water pressure and reduces the soil cohesion, ultimately complicating the situation. Implementing effective risk management strategies by encompassing both engineering solutions and community engagement is required. By fostering collaboration between scientists, engineers, and local communities, resilience against the landslides can be enhanced.

Abbreviations

ERT	Electrical Resistivity Tomography
MoHA	Ministry of Home Affairs
GPR	Ground Penetrating Radar

Acknowledgments

The authors would like to acknowledge Infrastructure Developent Office, Baglung and Explorer Geophysical Consultant Pvt. Ltd. for providing the data used in this study. We are grateful for their contribution to this research.

Conflict of Interest

The authors declare no conflicts of interest.

References

[1] Aleotti, P., & Chowdhury, R. (1999). Landslide hazard assessment: A review of methods and applications. *Bulletin of Engineering Geology and the Environment*, 58(1), 21-36.

[2] Bhattarai, B., & Sitaula, B. K. (2002). Landslide hazards in Nepal: An overview. *Natural Hazards*, 26(1), 29-49.

[3] Budha, P. B., & Chhetri, R. B. (2016). Geophysical techniques for subsurface investigation related to landslides. *Journal of Applied Geophysics*, 130, 50–60.

[4] Dangol, B. R. (2002). The impact of landslides on infrastructure in Nepal: A case study approach. *Journal of Mountain Science*, 4(1), 53-64.

[5] Department of Mines and Geology. (1985). Geological map of Western Nepal (Scale 1:250,000). Kathmandu, Nepal: Department of Mines and Geology.

[6] Ghimire, M., & Shrestha, S. (2010). Landslide risk assessment in Nepal: A case study from the hilly region of Nepal. *Landslides*, 7(3), 287-298.

[7] Hasegawa, S., & Dahal, R. K. (2009). Influence of lithology on landslide susceptibility in the Himalayan region of Nepal: A case study from the Lesser Himalaya of Nepal based on weights-of-evidence modeling approach. *Geomorphology*, 102(3-4), 496-510.

[8] Igwe, J. C. (2015). Soil mechanics and landslide prediction. *Landslide*s, 12(5), 733–743.

[9] Kayastha, P., Dhital, M. R., & De Smedt, F. (2012). Landslide susceptibility mapping using the weight of evidence method in the Tinau watershed, Nepal. *Natural hazards*, 63, 479-498.

[10] Kjekstad O., Highland L. M. (2009). Economic and Social Impacts of Landslides in Landslides–Disaster Risk Reduction; Springer: Berlin Heidelberg Germany.

[11] Melkamie, T., Adhikari, R., & Shrestha, S. B. (2024). Geotechnical characterization of landslides: A comprehensive study from Nepal's hilly regions. *Landslides.*

[12] Palacky, G. J. (1987). Conductivity-resistivity values of various rock-forming materials. Geophysical Research Letters, 14(11), 1291-1294. https://doi.org/10.1029/GL014i011p01291

[13] Petley D. N., Hearn G. J., Hart A., Rosser N. J., Dunning S. A., Oven K., Mitchell W. A. (2007). Trends in Landslide Occurrence in Nepal: *A Review. Geological Society Special Publications*, 273(1), 217–226.

[14] Poudyal, R., & Kafle, G. K. (2012). Community-based disaster risk management in Nepal: A case study of landslide-prone areas. *International Journal of Disaster Risk Reduction*, 2, 12-20.

[15] Sapkota, N., & Paudel, L. P. (2018). Geological study of the Lesser Himalaya in the Kusma - Baglung area, Western Nepal. Bulletin of the Department of Geology, 20, 29-36. https://doi.org/10.3126/bdg.v20i0.20721

[16] Sassa, K., & Takahashi, T. (2004). Geophysical methods for landslide investigation and monitoring: Applications in Japan and Nepal. *Landslides*, 1(1), 55-64.

[17] Tang, Y. (2023). Satellite imagery applications for landslide monitoring. *Remote Sensing Applications: Society and Environment*, 28, 100–110.

[18] Telford, W. M., Geldart, L. P., & Sheriff, R. E. (1990). Applied geophysics (2nd ed.). Cambridge University Press.

[19] Thapa P. B., Lamichhane S., Joshi K. P., Regmi A. R., Bhattarai D., Adhikari H. (2023). Landslide Susceptibility Assessment in Nepal’s Chure Region: A Geospatial Analysis. *Land*, 12(12), 2186.

[20] Upreti, B. The physiography and geology of Nepal and their bearing on the landslide problem. In Landslide Hazard Mitigation in the Hindu Kush-Himalayas; *International Centre for Integrated Mountain Development:* Kathmandu, Nepal, 2001; pp. 31–49.

[21] Wang, G., & Sassa, K. (2005). Shear strength parameters and their implications for landslide susceptibility. *Engineering Geology*, 81(3), 223–233.